Heliyon 10 (2024) e35828

Contents lists available at ScienceDirect

Heliyon

journal homepage: www.cell.com/heliyon

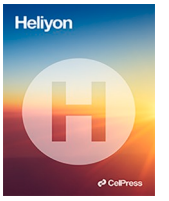

Research article

Facile synthesis of ZnO nanoparticles using *Nigella Sativa* extract and its role as catalyst in production of bio-oil and degradation of methylene blue dye

Huma Jamil [a,b,*], Muhammad Faizan [b,c]

[a] *Institute of Physical Chemistry, Polish Academy of Sciences, Kasprzaka 44/52, 01-224, Warsaw, Poland*
[b] *University of the Punjab, Lahore, Pakistan*
[c] *Technische Universität Chemnitz, Straße der Nationen 62, D-09111, Chemnitz, Germany*

ARTICLE INFO

Keywords:
Green synthesis
ZnO NPs
Pyrolysis
Bio-oil
Methylene blue
Catalytic degradation

ABSTRACT

Zinc Oxide (ZnO) nanoparticles (NPs) were synthesized using an environmentally benign biogenic approach employing an extract of kernels of *Nigella Sativa* (kalonji). The presence of primary and secondary metabolites in *Nigella Sativa* extract acted as the capping and reducing agent. The as-synthesized ZnO NPs were characterized using various advanced techniques i.e., UV, SEM, XRD, EDS, TGA, DSC, and FTIR spectra. UV characterization of ZnO NPs revealed a peak within the 350-400 cm^{-1} range, confirming their successful formation. XRD spectra revealed that the particles possess a nano-rods and platelets structure, with an average size of 65 nm. XRD analysis revealed that the particles possess a size of 65 nm with a nano-rods and platelets structure. FTIR spectra of the ZnO NPs exhibited a peak at a wavenumber range of 500–600 cm^{-1}. The newly fabricated ZnO NPs were utilized in a pyrolysis reaction for the production of high-yield bio-oil, resulting in a maximum yield of 65.6 % at 350 °C. The spectra of the bio-oil display distinct peaks at 1340 cm^{-1}, 2923.6 cm^{-1}, and 1617 cm^{-1}, which suggest the existence of phenolic and carbonyl chemicals. After incubating for 24 h under UV light, they also demonstrated significant catalytic degradation of methylene blue dye. The highest degradation was recorded to be an average of 71 % in 60 min of UV exposure. Taken together, ZnO NPs developed by eco-benign methods have the potential to be implemented as a novel catalytic system in the production of bio-oil as well as the remediation of dye-harboring industrial wastewater.

1. Introduction

The nano-technology field has the potential to manipulate matter at its nanoscale range, which creates materials that depict unique properties with versatile societal applications. Nanomaterials act as magic pills that contain chemicals, genes, or herbicides, pushing plant parts to release chemicals. Among these nanomaterials, ZnO NPs have gathered much attention from researchers owing to their versatility and applications such as sensors, electronics, environmental protection, communication, cosmetics, and medical and biological fields [1]. ZnO NPs belong to the metal oxide family with the most prominent characteristics in the field of photo-oxidation and photo-catalytic activity against biological and chemical species [1c]. ZnO is a renowned semiconductor that shows n-type properties with a bridge gap of 3.37 eV and a huge binding excitation energy of 60 meV. This has occupied a special place in different metal oxide

* Corresponding author. School of Chemistry, University of the Punjab, Lahore, Pakistan.
E-mail address: humajameel89@gmail.com (H. Jamil).

https://doi.org/10.1016/j.heliyon.2024.e35828
Received 3 April 2024; Received in revised form 2 August 2024; Accepted 5 August 2024
Available online 6 August 2024

nanomaterials because of its electrical, optical, and catalytic properties [2]. ZnO shows excellent gas sensing properties towards many gases. So, to improve gas sensing properties, researchers focused on improving its gas sensing ability by preparing ZnO with distinctive morphologies and verifying its surface properties with various metals [3].

There are different methods that have been utilized so far for the preparation of ZnO NPs which include hydrothermal, sol-gel, spray pyrolysis, precipitation method, ultrasonic condition, chemical vapor deposition and microwave assisted methods [4]. These preparation methods are hazardous, demand high input energy, involve the use of chemicals, are unsafe for the environment, and have environmental risks. In contrast, biological methods involve the use of microbes, algae, fungi, and plants, which involves lesser use of the chemicals that cause lesser environmental aberration and are considered eco-friendly. Using the microbes for NPs preparation is associated with various drawbacks which include longer required time and microbe screening, constant culture observation and shape and size of NPs [5]. However, micro and macro-algae are not explored much for the NPs preparation. In this article, we have utilized plant extract for nano-material preparation because plants contain various primary and secondary metabolites such as tannins, saponins, phenolic compounds, polypeptides, starch, flavonoids, and terpenoids which act as capping and reducing agents. As a result, Zn (II) in the salt solution can be capped and reduced and subsequent oxidizing, well dispersed and stable ZnO Nps are obtained. In order to extract these metabolites, mild solvents methanol, ethanol, or water are used, which react with zinc salt in various conditions, giving different yields [6]. Over the years, various plant have been used for this purpose such as *Calotropi sprocera* [7], *Aloe vera* [8], *Ocimum bacillius* [9], *Solanum nigrum, Agathosma betullina and Acacia caesia* [10], *Lagenaria siceraria* [11] *Vitex negundo* [12], *Camellia sinensis* [13], *Eucalyptus globulus* [14]. ZnO NPs are known as biocompatible, environmentally safe with array of applicability, which has swelled the curiosity of the scientist. These nanomaterials are used in drug delivery [15], in gas sensors as semiconductor nanomaterial [16], optoelectronic & electronic devices [17], photocatalysis [18], cosmetic products [19], pharmaceutical [20], water cleaning [21], self-cleaning fabrics [22] and as catalysts for yield improvement [23] and other chemical reactions [24].

In this article, *Nigella Sativa* (Kalonji) has been employed for the preparation of ZnO nano-particles. *Nigella Sativa* is generally well-known by names of black cumin or black seeds. Karnels of *Nigella Sativa* contain 0.4 %–2.5 % of essential oils, 36 %–38 % fixed oils, saponins, proteins, and alkaloids [25]. Pyrolysis is a process in which wood and lignocellulosic biomass are used for the production of energy in the form of bio-oil and syngas [26]. ZnO NPs are used in pyrolysis reactions as catalysts to enhance the yield of bio-oil. In this study, peels of *Punica granatum* (Pomegranate) used for the production of bio-oil through pyrolysis method. In the past years most of the pyrolysis work is focused on the usage of pulp and seeds of *Punica granatum* but a very few attempts were made to use peels for the energy production. In this work the peels of *Punica granatum* are implied for the cost-effective bio-oil generation with the addition of biologically synthesized ZnO catalyst and comparing the yield with standard catalyst Zeolite Socony Mobil # 5 (ZSM-5).

Globally, water pollution has become the major concern because it effects the biodiversity of our ecosystem critically leading to loss of life numerously owing to the contaminate water [27]. Industries play crucial role in this matter as their effluents cause liver damage, skin irritation, kidney failure, blood disorders, carcinogenic & mutagenic effects and poisoning of central nervous system [28]. For this purpose, it is imperative to eliminate synthetic dyes from the effluents. Methylene blue (MB) is one of the synthetic dye, which is water soluble leading to toxic effect on aquatic life and nitrifying bacteria [29]. The MB dye is bio-accumulated, non-biodegradable, and carcinogenic, which makes its degradation crucial. Due to having large surface along with quantum confinement resulting in photogenerated charge carrier for degradation of organic pollutants using UV/Vis light, it is said that semiconductor metal oxides can perform significant photocatalytic reduction [30]. For this purpose, ZnO NPs is the ideal contender for the MB dye degradation because they show excellent photocatalytic activity because of high surface area to volume ratio [31]. Because ZnO NPs show environmentally benign which is the reason they to be explored more to explore their potential applications which is crucial to bridge the research gap in the field of nanotechnology. These qualities make them best candidate for studying the photocatalytic degradation of organic pollutant and use them for the wastewater treatment. In this article we studied the photocatalytic ability of ZnO NPs prepared using *Nigella Sativa* along with pyrolysis.

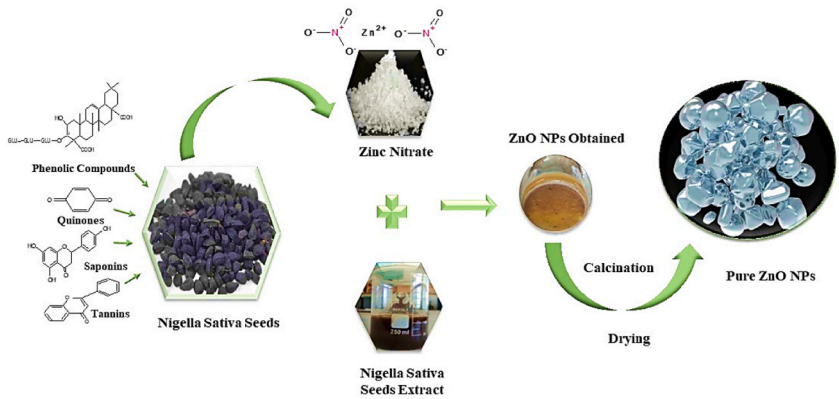

Fig. 1. ZnO NPs formation from *Nigella sativa* seeds.

2. Materials and methods

For the procedure, zinc nitrate hexahydrate ($Zn(NO_3)_2.6H_2O$), sodium hydroxide (NaOH), methanol (CH_3OH), ZSM-5, and MB dye were used, and all the chemicals were used Sigma Aldrich. All chemical were used in their pure form without further purification. In Pyrolysis reaction dried peels of *Punica granatum* were taken from nearby market in Lahore.

In this method, firstly we prepared the extract from *Nigella Sativa.* For that, 5 g quantity of fine powder of kernels of *N. Sativa* were dispersed in 40 % solution of Methanol (CH_3OH) and heated on hot plate at 90 °C for 60 min (Fig. 1). The seeds of *Nigella Sativa* are full of important anti-oxidants. So, in order to identify their presence, phytochemical analysis was done. They were done to check the presence of poly-phenolic compounds, reducing sugars, saponins, tannins and terpenoids. For NPs preparation, First, we prepared 1M $Zn(NO_3)_2$ and 1M solution of NaOH. Following that, in a 100 ml beaker 10 ml plant extract and 10 ml solution of $Zn(NO_3)_2$ was taken (1:1). In order to adjust the pH of the solution in the range of 12–13, 1M NaOH solution was used. After maintaining the pH of the solution, the reaction system was placed on the hot plate and reaction was carried out for 120 min at 90 °C. Obtained ZnO NPs were dried, calcined at 350 °C and used for characterization purposes.

2.1. Application of ZnO NPs in pyrolysis

Pyrolysis of *Punica Granatum* was done at various temperatures from 250 to 500 °C to set the optimum conditions. The optimization of the reactions gave maximum yield at a temperature of 350 °C. Further on, catalytic was loaded on the biomass by stirring the peel powder and 1 g of ZnO NPs in hot water for 10 min. After 10 min, the biomass filtered and dried to get rid of all the moisture and moved to pyrolysis reactor bio-oil. Same reaction was carried out with ZSM-5, at different catalytic conditions and the yield obtained in all the process was compared.

2.2. Application in dye degradation

Different concentrations of MB dye were prepared and the pH of the solutions were maintained at 12 using 1M sodium hydroxide (NaOH). After that, 0.1 g of the ZnO NPs catalyst were added in the dye samples and sonicated for 10 min. After attaining 24-h incubation period, all the samples were irradiated under UV–visible light until they showed maximum degradation of dye, which was recorded every 5 min.

2.3. Characterization

For the characterization of ZNO NPs UV (SPD-10A UV-VIS Detector With Longwave Variation/2118-AS/) in solid state under O_2 environment, FTIR (ATR adapter for FTIR Spectrophotometer (3009-AS) in solid state with 2 cm^{-1} with scan number 1024 and pressure of 6 hPa, XRD Mikroskop Meophat 2) under nitrogen environment, SEM & EDX (Inviumstah Potentiostat. with Multiplex and Control Unit, Software.) was done under vacuum and TGA from 20 to 1000 °C with heating rate of 5 °C/min & DSC (Kalorymetr TG-DSC 111) at 20–500 °C 5deg/min under N2 were performed. The characterization methods confirmed the formation of ZnO NPs and elucidated the structure and size of NPs.

3. Result and discussion

3.1. Phytochemical investigation of Nigella Sativa extract

Phytochemical exploration of the extract of *Nigella Sativa* kernels was accomplished to ascertain the existence of some compounds such as, saponins, tannins, poly-phenolic compounds reducing sugars and terpenoids. Obtained outcomes of the performed tests are given in Table 1.

Table 1
Phytochemical tests and their results.

Sr. #	Constituents	Test	Results
1	Poly-phenolic compounds	5 ml extract + 1 ml of $FeCl_3$ + 1 % solution of $K_3[Fe(CN)_6]$	Negative with no reddish blue colour formation
2	Reducing Sugar	5 ml extract + 5 ml Fehling solution A + 5 ml of Fehling solution B+ heat	Positive giving brick red ppt
3	Saponins	10 ml distilled H_2O+ 3 ml extract + shake for 30 min	Positive with honey comb formation
4	Tannins	3 ml extract+ 10 % alcoholic $FeCl_3$	Positive showing greenish grey or Dark blue colour
5	Terpenoids	5 ml extract + 2 ml $CHCl_3$ + 3 ml H_2SO_4	Negative with no reddish-brown interface between 2 layers

3.2. UV/visible analysis

UV/Vis spectra of the sample shows (Fig. 2(a)) the absorption peak fall in the area of 200–800 nm. In the spectra, ZnO NPs displayed their characteristic absorption peak in the range of 350–400 nm. Size and shape of NPs are the determining factors for the width and shape of absorption peak. The absorption peak near the region of 350–400 nm is an indicator of the synthesis of pure ZnO NPs that have high efficiency in absorbing ultraviolet radiation [32]. No other absorption peak observed in this region confirmed that the NPs formed are very pure [33]. Wide range of studies are available that exhibit that ZnO NPs display peaks in below 400 nm region. Similar results were reported by Zare et al., exhibiting the formation range of ZnO NPs formed by Thymus vulgaris leaf extract in the range of 270 nm [34], Wary et al. reported the preparation of ZnO NPs by using coconut husk give the absorption peak below 400 nm [35] and Bhuyan et al. prepared ZnO NPs using *Azadirachta indica* depicting the UV range of 377 nm [36]. The band gap energy of the ZnO NPs was calculated using Kubelka-Munk function $(\alpha h\nu)2 = A(h\nu\text{-}Eg)$, where α, hν, Eg, and A are the absorption coefficient, photon energy, band gap energy, and constant, respectively. In Fig. 2(b), it can be seen clearly that the band gap energy of ZnO NPs is 3.1 eV [37]. The small band gap energy is attributed to the consequence of the native defects (zinc interstitials and oxygen vacancies) resulting in the localized electronic states in the energy gap, which in turn give high efficiency of ZnO NPs in pyrolysis and photodegradation [38].

3.3. FTIR analysis

Fig. 3 (a) exhibited the FTIR spectra of ZnO compounds in the range of 4000–500 cm^{-1}. ZnO NPs exhibit its characteristics absorption peak in the range of 500–600 cm^{-1} [7,31,39]. However, the peak at 3544.94 cm^{-1} represents the stretching vibration of the hydroxyl group (OH) [40]. The absorption band in the region of 2923.24 cm^{-1} is associated with the C–H Stretching vibration [7,31, 36,39a,39b,40]. The range of 1634 cm^{-1} is associated with stretching vibration of C=C groups [41]. The vibration of OH, C=C and C–H group are belong to the reducing sugars, saponins and tannins that are present in the extract of *Nigella sativa,* which is used for the synthesis of the NPs.

3.4. X-Ray diffraction (XRD) analysis

The XRD pattern of as-synthesized ZnO NPs is shown in Fig. 3(b). The measurements were done in the range of 10–80° 2-theta and analyzed with Jade software. The data recorded provide the diffraction peaks at the 2-theta value of 31.78°, 34.40°, 36.28°, 47.50°, 56.44°, 62.80°, 67.86° respectively. The characteristic diffraction peaks of NPs are well indexed with hexagonal ZnO (JCPDS Card No. 36–1451). The ZnO NPs are mainly present in cubic zinc blends or hexagons [42]. More interestingly, the XRD pattern also confirms the high purity of the sample as all the diffraction signals correspond to ZnO NPs and it does not contain any signals other than that which is confirmed by EDS elemental mapping data (fig.S 2) that is clearly showing that peaks of no other elements were seen. This high purity of nano-powder can enhance its efficiency in different applications. Moreover, the height of the peaks indicates the high crystallinity of the materials calcined at 350 °C temperature. The Debye-Scherrer's equation was used to calculate the crystallite size of the material. In this equation D s crystallite size (nm), λ is the incident X-ray's wavelength, β is the full-width half maxima and θ is the diffraction angle.

$$D = \frac{0.89\lambda}{\beta \cos\theta}$$

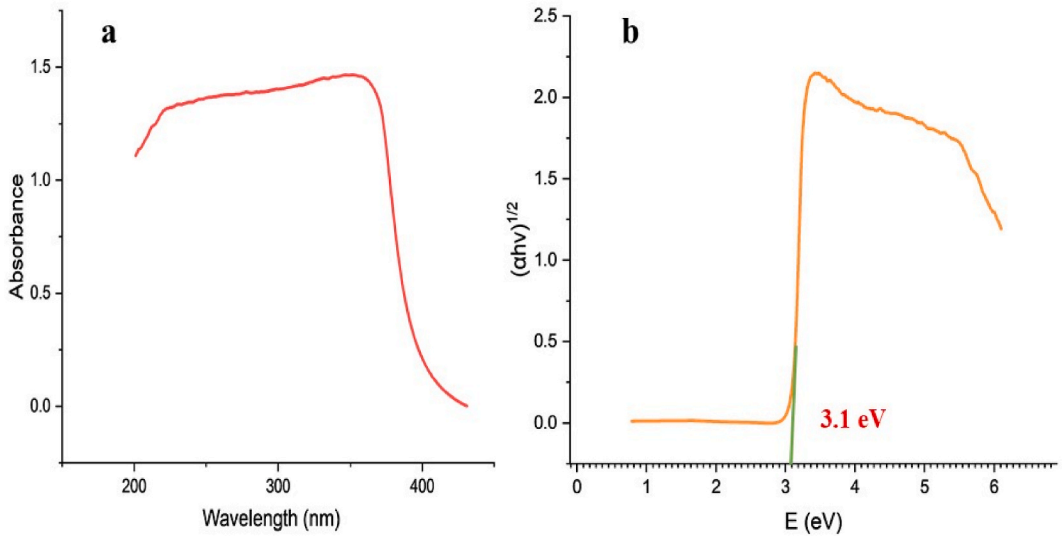

Fig. 2. (a) UV spectra of zinc oxide NPs and (b) is band gap energy of ZnO NPs.

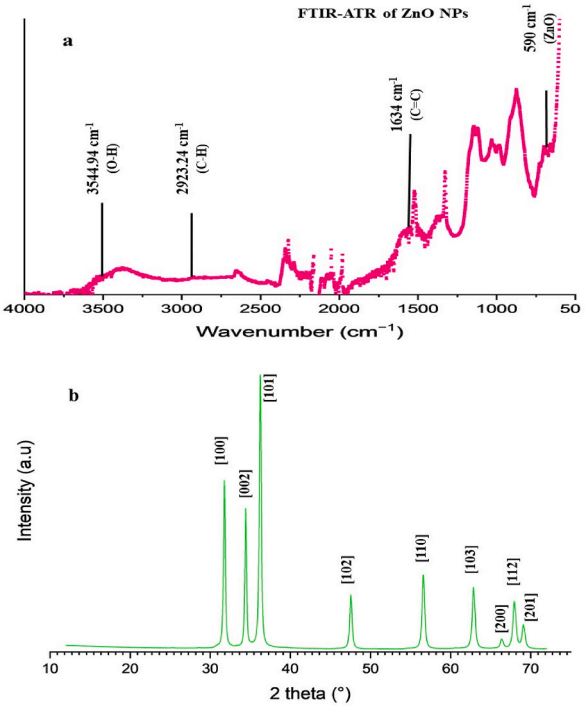

Fig. 3. FTIR (a) and XRD (b) pattern of biogenically synthesized ZnO NPs.

The crystallize size of ZnO NPs i.e., 65 nm was measured by using full-width half maxima of peaks at 31.78°, 34.40°, and 36.28° 2-theta values. The lattice parameters obtained after reitveld refinement were a = 3.242031 b = 3.242031 c = 5.193165. While Williammson Hall slope gave microstrain 5.46 × 10^{-3} with crystallite size of 65 nm. The Intercept calculated was 0.00199 m while slope was 0.00546 m.

3.5. SEM and EDS analysis $^{-1}$

Morphological characteristics of the ZnO NPs was done using SEM analysis. The SEM micrograph is given in Fig. 4 (a & b), which revealed the agglomeration, size, and shape distribution of the ZnO NPs. However, images revealed different shape of particles which dominantly comprised of nano-rods and platelet without adherence to each other. Similar results were reported in the literature [42b]. The average size of the particles seen in SEM analysis is in the range of 60–65 nm which coincide with the results obtained from XRD. The energy dispersive X-ray spectroscopy (EDS) mapping image of the biogenically prepared ZnO NPs confirmed the uniform and homogenous formation of ZnO NPs Fig. 4 (c, d, e and f) [43]. The EDS mapping also the content of carbon comes from the carbon tape while Al comes from the sample holder.

3.6. DSC and TGA of ZnO NPs

The Fig. 5 (a & b) depicts the typical DSC & TGA of the biologically synthesized ZnO NPs based on the heating process of 5 °C per minute. Thermo-gravimetric analysis includes the heat-induced decomposition of the material, which initiates bond breakage in the system under study [44]. The TGA profile showed 2 sharp changes with continued weight loss Fig. 5 (a). First peak appear at 180–200 °C region with 10 % weight loss which may be occurred due to the loss of water molecules which were physically adsorbed on the NPs. The peak observed at 550 °C, causing 30 % loss, is because of chemically absorbed alcohol, water, hydroxyl group and water which cause the formation of pure ZnO NPs [45]. In the DSC curve, two major peaks observed in the range of 80 °C and 300 °C is attributed to the probable loss of adsorbed volatile molecules on the surface of the NPs Fig. 5 (b). The peak at 300 °C is associated with the degradation of organic matter and the formation of ZnO NPs 300 °C [45].

3.7. Mechanism of formation of ZnO NPs

Phytochemicals present in the plant play crucial role in the synthesis of nanoparticles (Fig. 6). The probable mechanism for the formation of ZnO NPs is predicted as the zinc nitrate mixed with the extract of *Nigella sativa,* Zn^{2+} ions distribute thoroughly and uniformly in the extract and form the complex with the active agents. The resulting complex structure go through sluggish decomposition upon heat application. In a nutshell, the phytochemical helps in the reduction of Zn^{2+} ions, making ZnO NPs with a small size.

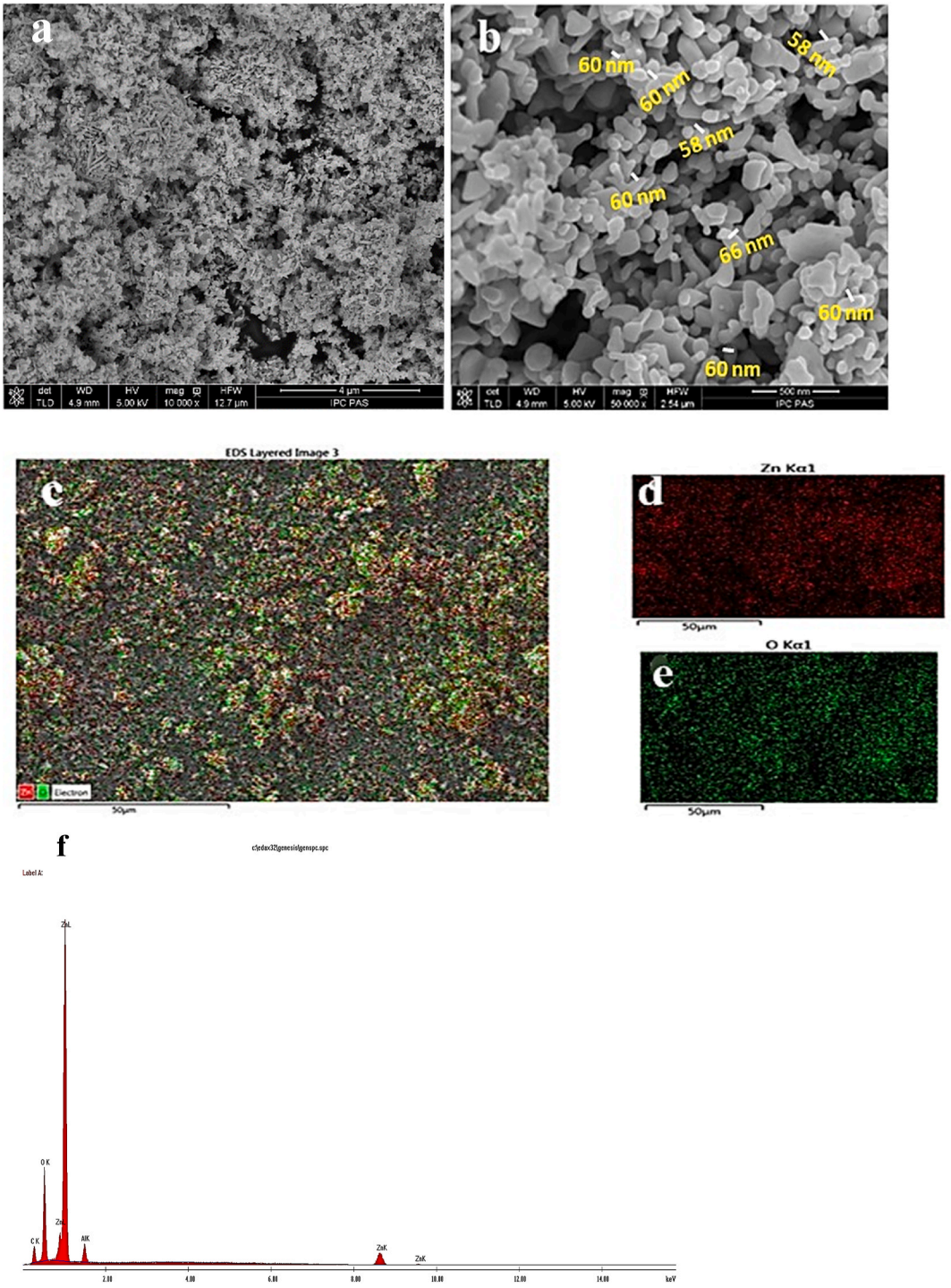

Fig. 4. Fig. a and b depict the SEM images of ZnO NPs while Fig, c, d, e, and f, and h depict EDS elemental mapping and graph.

3.8. Application of ZnO NPs in pyrolysis O_2

Pyrolysis reactions of pomegranate peels was performed in the fixed bed reactor with inflow of nitrogen to maintain the inert atmosphere and collecting bottles shown in Fig. 7. The reaction performed at various temperature range giving out varied ratios of charcoal, gas and oil. The obtained amount of the end-products are depicted in Table 2 and Fig. 8. The data clearly depicts that increasing temperature increases the syn-gas fraction of the product, and at 500 °C, syngas dominated the product yield. This coincides

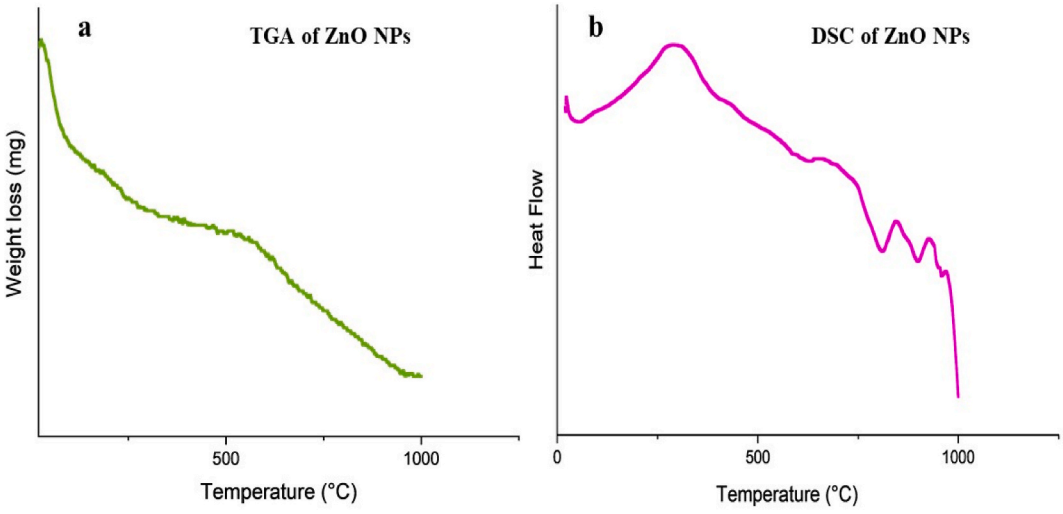

Fig. 5. TGA (a) and DSC (b) of ZnO NPs.

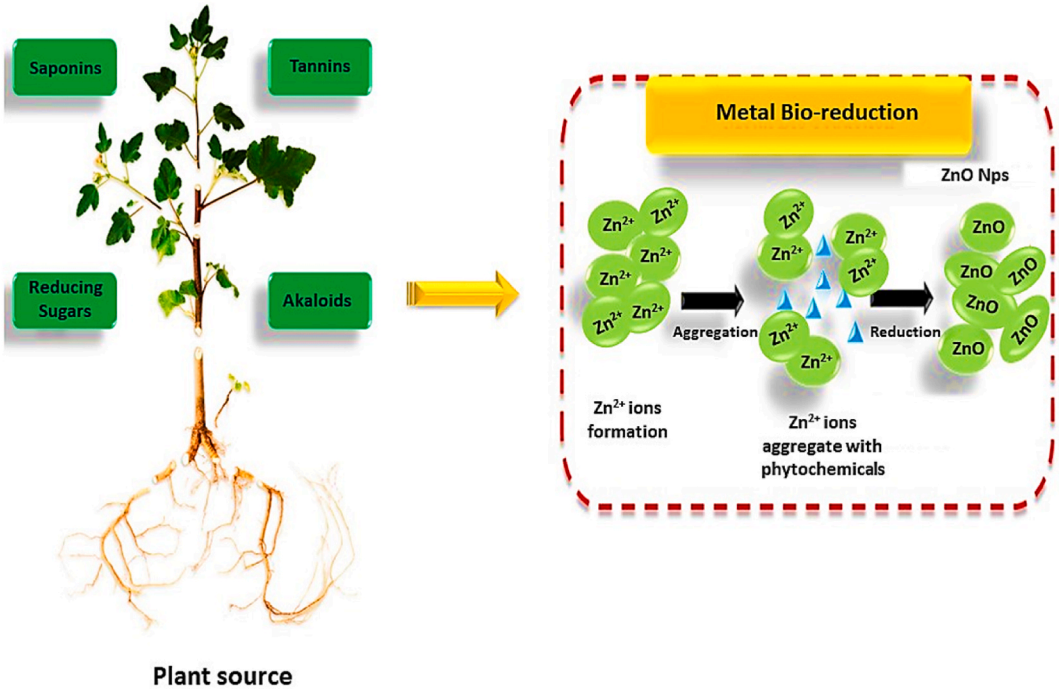

Fig. 6. Mechanism for the formation of ZnO NPs.

with the several studies which showed that higher temperature favours the formation of gas, while high heating rate gives bio-oil as the main product [46]. Table 3 and Fig. 9 exhibit another data of pyrolysis reaction after maintaining the reaction conditions. As it was clear from the previous set of reactions that pyrolysis of *Punica granatum* peels gave a maximum yield of bio-oil at 350 °C, the next set of reactions was performed with the inclusion of different catalysts after the catalyst loading. For this purpose, standard catalyst and biogenically prepared ZnO NPs loaded on the biomass. The amount produced from the reactions clearly exhibits that the ZnO catalyst gave maximum yield over ZSM-5, which is attributed to the low bandgap energy of the ZnO NPs.

In FT-IR analysis reveal that peak is seen in fig S (a, b and c) in the range of 2923.4 cm^{-1}, is associated with stretching vibration of CH_2 and CH_3 groups in carboxylic acid compounds while 1340 cm^{-1} region in all spectra is linked with its bending vibration. The band in 1617 cm^{-1} belongs to the stretching vibration of the carbonyl group [47]. The peak at 3394 cm^{-1} is linked with OH group of phenolic compounds while in fig. S (d) this OH peak disappeared due to high temperature given to the biomass and stretching band between 1450 and 1500 cm^{-1} belong to the N–H groups. However, in fig. S (b) the peak region between 700 and 800 is associated ZnO

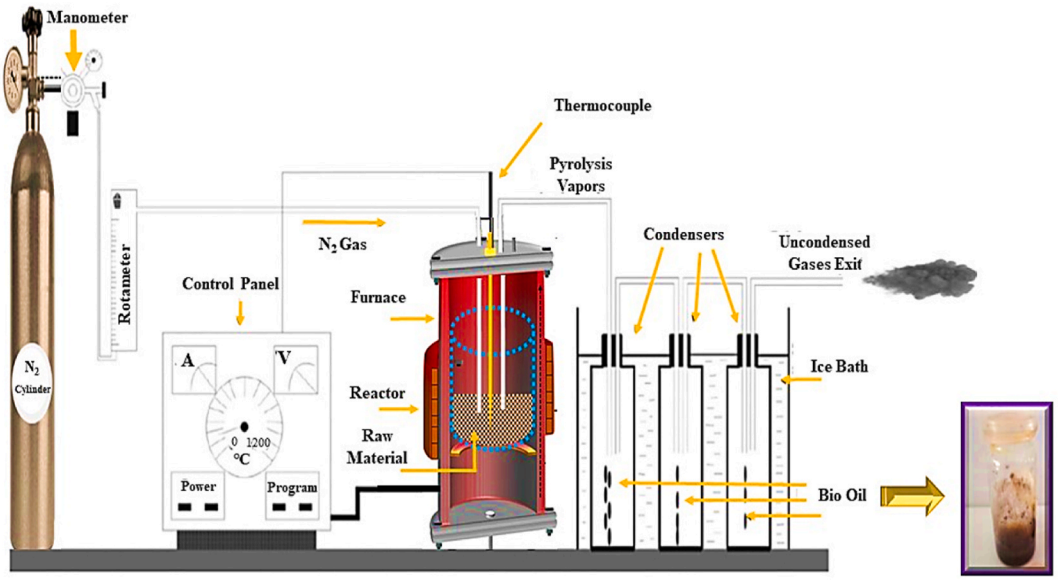

Fig. 7. Fixed bed pyrolysis reactor used for *Punica granatum* pyrolysis for the production of high yield bio-oil.

Table 2
Pyrolysis reaction at various temperatures and (%) yield of the end products.

Temperature (°C)	Time (mins)	Oil Yield (%)	Charcoal Yield (%)	Gas Yield (%)
300	19	34.8	29.6	35.6
350	18	44	22.4	33.6
400	10	38	32.7	28.4
450	8	37	34.0	28.5
500	10	30.9	24.9	44.2

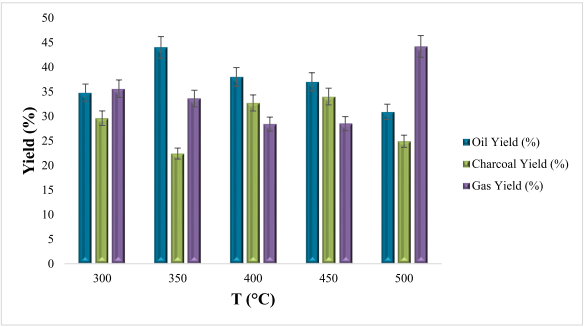

Fig. 8. Yield of products at different temperatures.

Table 3
Pyrolysis reaction product yield in various catalytic environment (T = 350 °C).

Constituents	Oil yield (%)	Charcoal yield (%)	Gas yield (%)
Without Catalyst	44	22.4	33.6
With ZnO catalyst	65.6	20.6	13.8
With ZSM-5	24	33	43

with is present in the biomass for after loading [48]. Peaks falling under the area of 300–380 cm-1 belong to the bending vibration of C–H, and peaks in the region of 1107 cm-1 are associated with stretching C stretching vibration, while peaks in the region of 1000 cm-1 belong to C stretching vibrations. The spectra gives us the idea of presence of important compounds, which are of chief importance in

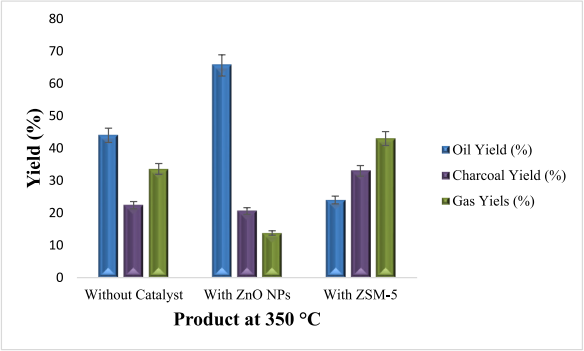

Fig. 9. Product yield with different catalytic environment.

determining the value of bio-oil.

Along with the bio-oil, the pyrolysis of the *Punica granatum* also gave char, which is an excellent abosrbant and can be used for the wastewater treatment as well.

3.9. Photocatalytic degradation

Photocatalytic activity of prepared ZnO NPs was evaluated by computing the rate of MB degradation, chosen as a model reaction [49].

Different concentrations of MB solutions (10, 20, 30, 40, and 50 ppm) were prepared in distilled water, followed by the preparation of ZnO NPs solution by dispersing the particles in the distilled by means of sonication in a water bath for 10 min to ensure complete and thorough mixing. The reaction blends were prepared by adding varied quantities of NPs suspension to the aqueous solution of MB dye and 1M solution of NaOH to maintain the pH at 12.0. Afterward, samples were placed in incubation for 24 h at room temperature in order to attain the adsorption-desorption equilibrium for MB on the catalyst surface. After attainment of equilibrium, 1.0 mL of sample was extracted to examine the initial concentration (C_0) of MB solution, and the remaining mix was irradiated with a UV–Vis lamp to initiate dye degradation. The distance between the sample mix and radiation source was nearly 25 cm. At specific time breaks, sample mix (1.0 mL) was taken out and centrifuged immediately to eliminate the photocatalytic particles. The supernatant was then analyzed by UV-VIS spectrophotometer with absorbance measurements range of 250–650 nm to analyze the concentration of MB at every time lapse (5 min), which is denoted as C_t. The calibration curves of MB were analyzed showing the linear pattern in the range of 1.0–25.0 mg/L ($y = 0.0781x + 0.0083$; $R^2 = 0.9999$).

The catalytic degradation efficiency was calculated using the following equation [1]:

$$\text{Decolorization efficiency (\%)} = (A_0\text{-}A)/A_0 \text{ x } 100 \quad [1]$$

Where A_0 is the absorbance of MB dye solution prior to the irradiation, A is the absorbance of MB solutions in reaction mixture afterward time t. The unirradiated samples and MB solutions without NPs were utilized for comparison. For the photocatalytic degradation of MB dye was illustrated through pseudo first Kinetic model utilizing the following equation [2]:

$$\log C_0/C_t = kt \quad [2]$$

Where C_0 is the initial concentration of MB while C_t represents the sample at time *t* after irradiation, respectively, while *k* is rate constant [50]. The added solution of NaOH which maintained the pH of the solution helped increasing the efficiency of the photocatalytic degradation of ZnO NPs. The results of catalytic degradation showed promising results with 71 % of dye degraded in just 60 min after the UV exposure (Fig. 11). Fig. 10 shows the mechanism of degradation of MB dye. The photocatalytic mechanism involve generation of electron hole pair following the separation of electron hole pair and oxidation reduction reaction on the surface of nanocatalyst which in turn generate highly reactive hydroxyl radical (·OH) Electrons in the conduction band of ZnO fall short of $O_2/\bullet O_2$ potential. Conduction band electrons of ZnO rarely interact with O_2 in the surrounding. ZnO transmits the O_2 when unbound electrons present in the catalyst interact with O_2. Comparing the potential of valence band of ZnO, the reduction potential of H_2O/OH and OH/OH is lower. This is the reason photocatalytic degradation occurs. Holes of the ZnO catalyst interact with H2O and OH, forming large amounts of OH [51]. Table 4. Shows the photocatalytic activity of ZnO NPs prepared using different plant extracts.

From the above section it is clear that, in the present study, prepared ZnO NPs show comparable photocatalytic activity by degrading 71 % of MB dye in less required time. This result shows the significant efficiency of the prepared ZnO NPs.

4. Future perspective

The green route provides for application driven synthesis of ZnO NPs. Studies have proven that green synthesis is novel, economic and is significantly efficient method for the synthesis of nanomaterials. Green synthesis of ZnO NPs is highly potential methods with

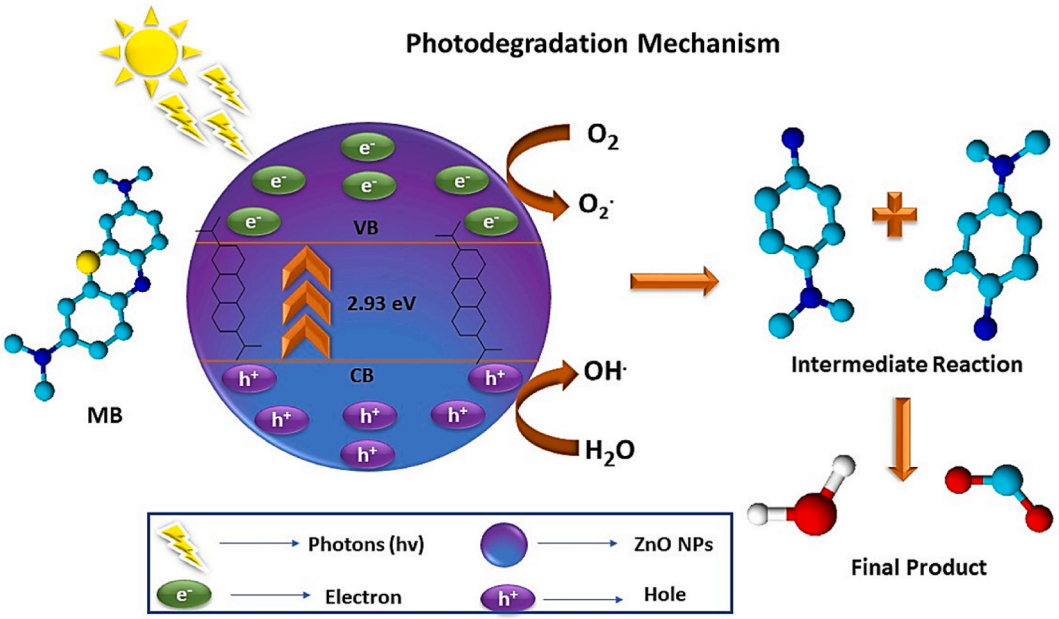

Fig. 10. Catalytic degradation mechanism of MB dye by ZnO NPs.

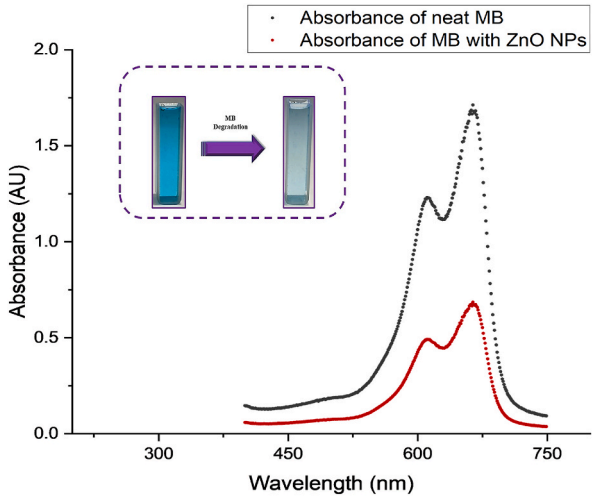

Fig. 11. Degradation of MB dye using ZnO NPs.

which we can control the size and morphology of the Zno NPs, which can be utilized for the further application in various fields such as agriculture, paints, semiconductors, biomedical, cosmetics and ecological fields to name few. Green approach is vastly favored owing to the utilization of plant components that leads to reaction, which needs mild conditions, low cost and less harmful byproducts. This green route is immensely aligned with the objectives of technology and nanoscience for the promotion of sustainable development and future prospects for improvement in ZnO, which will cover more aspects of the applications that are yet to be explored.

5. Conclusion

Phytochemicals in *Nigella sativa* assisted the formation of ZnO NPs with UV characterization depicted peak in the range of 350–400 cm^{-1} and particle size of 65 nm calculated by XRD & SEM exhibiting nano-rods and platelets structure while FTIR spectra of the ZnO NPs depicted the peak value of 500–600 cm^{-1}. XRD showed the lattice parameters obtained after reitveld refinement were a = 3.242031 b = 3.242031 c = 5.193165. The spectra of bio-oil depict the peak of phenolic group peaks and carbonyl group peaks predominantly in the area of 1340 cm^{-1}, 2923.6 cm^{-1} and 1617 cm^{-1} showing that bio-oil is made of comprised of carbonyl and phenolic compounds and in the spectra of charcoal this phenolic peak disappeared due to high temperature. Pyrolysis of *Punica*

Table 4
Photocatalytic degradation of MB dye by ZnO NPs prepared using different plant extract.

Plant	Dye	Photodegradation (%age)	Time (mins)	Reference
Coconut husk extract	MB and MY	97	100	[52]
Scutellaria baicalensis	MB	98.6 %	210	[53]
Trigonella foenum	MB	88.7 %	90	[54]
Citrus jambhiri lushi	MB	96	120	[55]
Ruellia tuberosa	MB & MG	94 & 92	150	[56]
Jujube fruit	MB	92	300	[57]
Syzygium Cumini	MB	91.4	180	[58]
Phoenix roebelenii	MB	98 %	105	[38]
Gomphrena serrata	MB	90.5 %	180	[59]
Acalypha indica	MB	96	90	[60]
Nigella Sativa	MB	71 %	60	Present study

Abbreviation: Metanil Yellow (MY), Malachite Green (MG).

granatum peels gave maximum yield at 350 °C, and loading of ZnO NPs catalyst enhanced bio-oil yield to 65.6 %. ZnO NPs also gave promising degradation results with MB dye, with an average dye degradation of 71 % in 60 min.

Data availability statement

The data will be available on request.

CRediT authorship contribution statement

Huma Jamil: Writing – review & editing, Writing – original draft, Visualization, Project administration, Investigation, Formal analysis, Data curation, Conceptualization. **Muhammad Faizan:** Writing – review & editing, Investigation, Formal analysis.

Declaration of competing interest

The authors declare the following financial interests/personal relationships which may be considered as potential competing interests:Huma Jamil reports article publishing charges was provided by Institute of Physical Chemistry Polish Academy of Sciences. If there are other authors, they declare that they have no known competing financial interests or personal relationships that could have appeared to influence the work reported in this paper.

References

[1] a) J. Hussein, M. El-Banna, T.A. Razik, M.E. El-Naggar, Int. J. Biol. Macromol. 107 (2018) 748;
b) L. Wang, Y. Kang, X. Liu, S. Zhang, W. Huang, S. Wang, Sensor. Actuator. B Chem. 162 (2012) 237;
c) M.M. Chikkanna, S.E. Neelagund, K.K. Rajashekarappa, SN Appl. Sci. 1 (2019) 117.
[2] R. Kumar, A. Umar, G. Kumar, H.S. Nalwa, A. Kumar, M. Akhtar, J. Mater. Sci. 52 (2017) 4743.
[3] F. Buazar, M. Bavi, F. Kroushawi, M. Halvani, A. Khaledi-Nasab, S. Hossieni, J. Exp. Nanosci. 11 (2016) 175.
[4] a) K. Omri, I. Najeh, R. Dhahri, J. El Ghoul, L. El Mir, Microelectron. Eng. 128 (2014) 53;
b) A.K. Zak, M.E. Abrishami, W.A. Majid, R. Yousefi, S. Hosseini, Ceram. Int. 37 (2011) 393;
c) C.-H. Lu, C.-H. Yeh, Ceram. Int. 26 (2000) 351;
d) K. Okuyama, I.W. Lenggoro, Chem. Eng. Sci. 58 (2003) 537;
e) J.J. Wu, S.C. Liu, Adv. Mater. 14 (2002) 215;
f) Y.-L. Wei, P.-C. Chang, J. Phys. Chem. Solid. 69 (2008) 688;
g) Y. Wang, C. Zhang, S. Bi, G. Luo, Powder Technol. 202 (2010) 130.
[5] F. Islam, S. Shohag, M.J. Uddin, M.R. Islam, M.H. Nafady, A. Akter, S. Mitra, A. Roy, T.B. Emran, S. Cavalu, Materials 15 (2022) 2160.
[6] S.M. Roopan, V. Devi Rajeswari, V. Kalpana, G. Elango, Appl. Microbiol. Biotechnol. 100 (2016) 1153.
[7] G. Sangeetha, S. Rajeshwari, R. Venckatesh, Mater. Res. Bull. 46 (2011) 2560.
[8] A. Chaudhary, N. Kumar, R. Kumar, R.K. Salar, SN Appl. Sci. 1 (2019) 1.
[9] H.A. Salam, R. Sivaraj, R. Venckatesh, Mater. Lett. 131 (2014) 16.
[10] a) M. Ramesh, M. Anbuvannan, G. Viruthagiri, Spectrochim. Acta Mol. Biomol. Spectrosc. 136 (2015) 864;
b) F. Thema, E. Manikandan, M. Dhlamini, M. Maaza, Mater. Lett. 161 (2015) 124;
c) J. Ashwini, T.R. Aswathy, A.B. Rahul, G.M. Thara, A.S. Nair, Catalysts 11 (2021) 1507.
[11] V. Kalpana, C. Payel, V.D. Rajeswari, Research Journal of Chemistry and Environment 21 (2017) 14.
[12] S. Ambika, M. Sundrarajan, J. Photochem. Photobiol. B Biol. 146 (2015) 52.
[13] O. Nava, P. Luque, C. Gómez-Gutiérrez, A. Vilchis-Nestor, A. Castro-Beltrán, M. Mota-González, A. Olivas, J. Mol. Struct. 1134 (2017) 121.
[14] B. Siripireddy, B.K. Mandal, Adv. Powder Technol. 28 (2017) 785.
[15] M. Stan, A. Popa, D. Toloman, T.-D. Silipas, D.C. Vodnar, Acta Metall. Sin. 29 (2016) 228.
[16] G. Umadevi, K.G. Krishna, Sensor Actuator Phys. 374 (2024) 115479.
[17] S.W. Balogun, H.O. Oyeshola, A.S. Ajani, O.O. James, M.K. Awodele, H.K. Adewumi, G.A. Àlàgbé, O. Olabisi, O.S. Akanbi, F.A. Ojeniyi, Heliyon 10 (2024) e29452.
[18] C. Ragavendran, C. Kamaraj, K. Jothimani, A. Priyadharsan, D.A. Kumar, D. Natarajan, G. Malafaia, Sustainable Materials and Technologies 36 (2023) e00597.
[19] R. Hamed, R.Z. Obeid, R. Abu-Huwaij, Nanotechnol. Rev. 12 (2023) 20230112.
[20] S. Maher, S. Nisar, S.M. Aslam, F. Saleem, F. Behlil, M. Imran, M.A. Assiri, A. Nouroz, N. Naheed, Z.A. Khan, ACS Omega 8 (2023) 15920.
[21] N. Bhattacharjee, I. Som, R. Saha, S. Mondal, Int. J. Environ. Anal. Chem. 104 (2024) 489.

[22] B.K. Dejene, T.M. Geletaw, Research Journal of Textile and Apparel, 2023.
[23] M. Akmal, A. Younus, A. Wakeel, Y. Jamil, M.A. Rashid, J. Plant Nutr. 46 (2023) 1077.
[24] A. Fouda, E. Saied, A.M. Eid, F. Kouadri, A.M. Alemam, M.F. Hamza, M. Alharbi, A. Elkelish, S.E.-D. Hassan, J. Funct. Biomater. 14 (2023) 205.
[25] B. Ali, G. Blunden, Phytotherapy Research: an International Journal Devoted to Pharmacological and Toxicological Evaluation of Natural Product Derivatives, vol. 17, 2003, p. 299.
[26] R.M.H.R. Shahruzzaman, S. Ali, R. Yunus, T.Y. Yun-Hin, Bulletin of Chemical Reaction Engineering & Catalysis, vol. 13, 2018, p. 489.
[27] P. Bautista, A. Mohedano, J. Casas, J. Zazo, J. Rodriguez, J. Chem. Technol. Biotechnol.: International Research in Process, Environmental & Clean Technology 83 (2008) 1323.
[28] A. Gürses, M. Açıkyıldız, K. Güneş, M.S. Gürses, A. Gürses, M. Açıkyıldız, K. Güneş, M.S. Gürses, Dyes Pigments 13 (2016).
[29] a) R. Atchudan, T.N.J.I. Edison, S. Perumal, D. Karthikeyan, Y.R. Lee, J. Photochem. Photobiol. B Biol. 162 (2016) 500;
b) R. Atchudan, T.N.J.I. Edison, S. Perumal, N. Karthik, D. Karthikeyan, M. Shanmugam, Y.R. Lee, J. Photochem. Photobiol. Chem. 350 (2018) 75.
[30] a) M. Curri, R. Comparelli, P.D. Cozzoli, G. Mascolo, A. Agostiano, Mater. Sci. Eng. C 23 (2003) 285;
b) S. Chakrabarti, B.K. Dutta, J. Hazard Mater. 112 (2004) 269.
[31] J. Lu, I. Batjikh, J. Hurh, Y. Han, H. Ali, R. Mathiyalagan, C. Ling, J.C. Ahn, D.C. Yang, Optik 182 (2019) 980.
[32] C. Soto-Robles, P. Luque, C. Gómez-Gutiérrez, O. Nava, A. Vilchis-Nestor, E. Lugo-Medina, R. Ranjithkumar, A. Castro-Beltrán, Results Phys. 15 (2019) 102807.
[33] a) R. Wahab, S. Ansari, Y.S. Kim, H.-K. Seo, G. Kim, G. Khang, H.-S. Shin, Mater. Res. Bull. 42 (2007) 1640;
b) R. Wahab, S. Ansari, Y.S. Kim, M. Dar, H.-S. Shin, J. Alloys Compd. 461 (2008) 66.
[34] M. Zare, K. Namratha, M. Thakur, K. Byrappa, Mater. Res. Bull. 109 (2019) 49.
[35] R.R. Wary, S. Baglari, D. Brahma, U.K. Gautam, P. Kalita, M.B. Baruah, Environ. Sci. Pollut. Control Ser. 29 (2022) 42837.
[36] T. Bhuyan, K. Mishra, M. Khanuja, R. Prasad, A. Varma, Mater. Sci. Semicond. Process. 32 (2015) 55.
[37] S. Yu, H. Zhang, J. Zhang, Z. Li, Sensors 19 (2019) 5267.
[38] T.S. Aldeen, H.E.A. Mohamed, M. Maaza, J. Phys. Chem. Solid. 160 (2022) 110313.
[39] a) P. Rajiv, S. Rajeshwari, R. Venckatesh, Spectrochim. Acta Mol. Biomol. Spectrosc. 112 (2013) 384;
b) C. Vani, G. Sergin, A. Annamalai, Int. J. Pharma Bio Sci. 2 (2011) 326;
c) W.J. Kim, V. Soshnikova, J. Markus, K.H. Oh, G. Anandapadmanaban, R. Mathiyalagan, Z.E.J. Perez, Y.J. Kim, D.C. Yang, Optik 178 (2019) 664.
[40] N.S. Rao, M.B. Rao, Am. J. Mater. Sci. 5 (2015) 66.
[41] S. Bashir, M.S. Awan, M.A. Farrukh, R. Naidu, S.A. Khan, N. Rafique, S. Ali, I. Hayat, I. Hussain, M.Z. Khan, Int. J. Nanomed. 17 (2022) 4073.
[42] a) Z. Obeizi, H. Benbouzid, S. Ouchenane, D. Yılmaz, M. Culha, M. Bououdina, Mater. Today Commun. 25 (2020) 101553;
b) R. Rathnasamy, P. Thangasamy, R. Thangamuthu, S. Sampath, V. Alagan, J. Mater. Sci. Mater. Electron. 28 (2017) 10374.
[43] a) H.B. Dias, M.I.B. Bernardi, V.S. Marangoni, A.C. de Abreu Bernardi, A.N. de Souza Rastelli, A.C. Hernandes, Mater. Sci. Eng. C 96 (2019) 391;
b) K.M. Rao, M. Suneetha, G.T. Park, A.G. Babu, S.S. Han, Int. J. Biol. Macromol. 155 (2020) 71;
c) K.A. Sultana, M.T. Islam, J.A. Silva, R.S. Turley, J.A. Hernandez-Viezcas, J.L. Gardea-Torresdey, J.C. Noveron, J. Mol. Liq. 307 (2020) 112931.
[44] Z.K. Shinwari, M. Maaza, Arch. Med. 3 (2017) 9.
[45] a) N. Matinise, X. Fuku, K. Kaviyarasu, N. Mayedwa, M. Maaza, Appl. Surf. Sci. 406 (2017) 339;
b) F.A. El-Kader, N. Hakeem, I. Elashmawi, A. Ismail, Aust. J. Basic Appl. Sci 7 (2013) 608.
[46] a) B. Av, *P*rogress in Thermochemical Biomass Conversion, 2001, p. 977;
b) C. Greenhalf, D. Nowakowski, A. Harms, J. Titiloye, A. Bridgwater, Fuel 108 (2013) 216.
[47] Ç.Ö. Ay, A.S. Özcan, Y. Erdoğan, A. Özcan, Colloids Surf. B Biointerfaces 100 (2012) 197.
[48] R. Sathyavathi, M.B. Krishna, S.V. Rao, R. Saritha, D.N. Rao, Adv. Sci. Lett. 3 (2010) 138.
[49] B.H. Masoum, A. Rezaei, A. NASIRI, 2009.
[50] K.A. Isai, V.S. Shrivastava, SN Appl. Sci. 1 (2019) 1.
[51] N. Chauhan, N. Thakur, A. Kumari, C. Khatana, R. Sharma, South Afr. J. Bot. 153 (2023) 370.
[52] S.S. Priyadharshini, J.P. Shubha, J. Shivalingappa, S.F. Adil, M. Kuniyil, M.R. Hatshan, B. Shaik, K. Kavalli, Crystals 12 (2021) 22.
[53] L. Chen, I. Batjikh, J. Hurh, Y. Han, Y. Huo, H. Ali, J.F. Li, E.J. Rupa, J.C. Ahn, R. Mathiyalagan, Optik 184 (2019) 324.
[54] A.A. Alshehri, M.A. Malik, J. Mater. Sci. Mater. Electron. 30 (2019) 16156.
[55] S. Waseem, T. Sittar, Z.N. Kayani, S. Gillani, M. Rafique, M.A. Nawaz, S.M. Shaheen, M.A. Assiri, Phys. B Condens. Matter 663 (2023) 415005.
[56] S. Vasantharaj, S. Sathiyavimal, P. Senthilkumar, V. Kalpana, G. Rajalakshmi, M. Alsehli, A. Elfasakhany, A. Pugazhendhi, J. Environ. Chem. Eng. 9 (2021) 105772.
[57] M. Golmohammadi, M. Honarmand, S. Ghanbari, Spectrochim. Acta Mol. Biomol. Spectrosc. 229 (2020) 117961.
[58] H. Sadiq, F. Sher, S. Sehar, E.C. Lima, S. Zhang, H.M. Iqbal, F. Zafar, M. Nuhanović, J. Mol. Liq. 335 (2021) 116567.
[59] A. Ramasubramanian, V. Selvaraj, P. Chinnathambi, S. Hussain, D. Ali, G. Kumar, P. Balaji, S. Sagadevan, Biomass Conversion and Biorefinery 13 (2023) 17271.
[60] G. Kamarajan, D.B. Anburaj, V. Porkalai, A. Muthuvel, G. Nedunchezhian, J. Indian Chem. Soc. 99 (2022) 100695.